Comparison of Thorax Responses between the Belted Elderly Occupant Human Body and THOR-50M FE Models under Typical Frontal Crash Test Conditions

Kazuki Hikida, Kazunori Maehara, Hidenori Mikami, Yasuhiro Dokko
Honda R&D Co., Ltd. Automobile R&D Center
Japan

Kazuki Ohhashi
Honda Techno Fort Co., Ltd Affiliation or Company Name
Japan

Paper Number 19-0172

ABSTRACT

In Japan the ratio of traffic accident fatalities of elderly people has been increasing, and the main factor is thorax injury. An elderly human body model (HBM) has been developed to evaluate the vehicle safety systems. At the same time, Test device for Human Occupant Restraint (THOR) ATD that has high bio-fidelity is being used in frontal crash tests including lateral vehicle motion. This paper describes the comparison of the thorax response between an elderly human and THOR 50th percentile male (THOR-50M) under a simulated frontal crash including lateral vehicle motion, and clarifies whether there is the correlation between them, especially, the correlation between the rib fractures of the elderly HBM and the thorax deformation of the THOR-50M.

The elderly HBM and THOR-50M model were compared under the condition of a driver seat position in a left-handed midsized sedan vehicle equipped with a three-point seat belt, a driver airbag, a knee airbag, and a side curtain airbag. The frontal crash motions of Full Width Rigid Barrier (FWRB) at 56 km/h, Offset Deformable Barrier (ODB) at 64 km/h, Small Overlap Test (SOT) at 64 km/h and Oblique Moving Deformable Barrier (OMDB)-to-vehicle crash test at 90 km/h were applied. From the results the thorax responses and deformation were investigated respectively.

The kinematics of each body component was in same trend between the elderly HBM and THOR-50M model in each test condition. For the elderly HBM and THOR-50M model in all the test conditions, the thorax deformation at the upper right was largest among four measurement locations, and that of the elderly HBM and THOR-50M model showed good correlation. In the elderly HBM, the locations of rib fractures were roughly assorted into three regions on the ribcage. The upper left ribs around the belt path in all test conditions, the right ribs around the belt path in FWRB and OMDB, and the lower left ribs in SOT and OMDB were fractured. The R^2 (correlation coefficient) between the number of fractured ribs of the elderly HBM and the overall peak resultant deformation (R_{max}) of THOR-50M was high as 0.83 for total rib fractures over all regions, while that wasn't high as 0.7 or less for those of each region.

The structural differences between the elderly human and THOR-50M such as the ribcage, spine and shoulder were considered to affect the differences of the kinematics and thorax deformation between them under frontal loading with lateral and vertical input.

The comparison results showed a certain correlation between the rib fractures of the elderly HBM and the thorax deformation of THOR-50M, and several differences of the partial thorax responses due to structural differences between humans and THOR-50M. The results of this study suggested that further study for the methods to evaluate detailed thorax injury using THOR-50M should be needed in order to correlate any other indices and possible thorax injuries in the crash conditions with lateral motion.

RESEARCH QUESTION/OBJECTIVE

In recent years, the population ratio of the elderly has been drastically increasing in developed countries such as Japan. Therefore, a lot of the elderly get caught up in traffic accidents. In Japan, the number of traffic accidents has been decreasing. However, the ratio of traffic accident fatalities of elderly people (aged 65 years old and older) has been increasing [1]. The thorax injury due to rib fractures is the main factor of the death of elderly people [2], because the density and strength of bone decrease with age [3]. It is necessary to evaluate the vehicle safety systems for the elderly occupant. Therefore the elderly occupant full body finite element (FE) models were developed to simulate vehicle occupant with restraint systems.

Anthropomorphic Test Device (ATD) has been used for assessing injury values in various countries. The bio-fidelity and measurement capability of ATD has been continuously improved. Test device for Human Occupant Restraint (THOR) ATD is considered to be the next-generation ATD in place of the traditional Hybrid III ATD. In THOR 50th Male (THOR-50M) ATD, the bio-fidelity had been enhanced to simulate human body in response to impact loading by using bio-mechanical data [4] [5]. Especially, the thoracic spine consists of a flexible rubber link and the rib cage has been redesigned to reproduce human rib geometry and structure. In addition, THOR-50M ATD is capable to measure the 3D thorax deformation at four locations with light reflective displacement meter which called the Infra-Red Telescoping Rod for Assessment of Chest Compression (IR-TRACC). Also, THOR-50M FE model has been developed to study the physical mechanical systems.

Some studies were conducted to evaluate the bio-fidelity of THOR-50M ATD in a simulated frontal crash [6] [7]. Recently, Albert et al. [10] showed the improved bio-fidelity of THOR-50M's thorax deformation by comparisons with the Hybrid III ATD and the elderly post-mortem human surrogates (PMHS) in frontal sled tests remarking the overall peak resultant thorax deformation, R_{max}.

For the purpose of reducing traffic fatalities of elderly people, an index to assess the thorax injury of elderly people in detail is necessary. It has not been thoroughly investigated whether the thorax injury of an elderly human under frontal crash including lateral motion can be assessed by THOR-50M ATD yet. This research compared the thorax response between elderly human and THOR-50M ATD under simulated frontal crash including lateral vehicle motion, and clarified whether there is a correlation between them, especially, a correlation between rib fractures of the elderly HBM and the thorax deformation of THOR-50M.

METHODS

Figure 1 (a) shows the elderly occupant full body FE model that is capable of predicting rib fracture, developed by Ito et al.[8] [9] and Dokko et al.[10] [11]. The model was designed to be a representative of elderly humans with an average American male body size (AM50%ile). The age of the elderly occupant FE model was defined as 75 years old. Rib fracture is predicted by 'element elimination' when an element strain reaches the specified fracture strain level. Figure 1 (b) shows the THOR-50th Metric FE model Version 1.4.1 developed by Humanetics Innovative Solution, Inc. [12]. LS-DYNA (Version971 R6.1.2) was adopted as a FEM solver [13].

(a) Elderly occupant full body FE model (b) THOR-50th Metric FE model Version 1.4.1

Figure 1. AM50 occupant FE models

As shown in Fig. 2 (1), in the full vehicle FE model, the elderly HBM and THOR-50M models were seated at the driver seat position of a left-handed midsized sedan vehicle. The simulated vehicle was equipped with a three-point seat belt that had a force limiter, a driver airbag, an outer anchor and a retractor pretensioner, a knee airbag and a side curtain airbag. Figure 2 (2) shows the shoulder belt path on the thorax of the elderly HBM and THOR model. The frontal crash motions of Full Width Rigid Barrier (FWRB) at 56 km/h, Offset Deformable Barrier (ODB) at 64 km/h, Small Overlap Test (SOT) at 64 km/h and Oblique Moving Deformable Barrier (OMDB)-to-vehicle test at 90 km/h were applied. The 6-axis motion of each test condition was made from the data of real collision test results. These models were simulated without the body deformation of a vehicle.

(1-a) Elderly HBM (1-b) THOR-50M model (2-a) Elderly HBM (2-b) THOR-50M model

Figure 2. Occupant and shoulder belt path on the thorax in full vehicle FE models

The elderly HBM and the THOR-50M models were seated at the same position as according to THOR-50M seating procedure [14]. Figure 3 shows the postures of the elderly HBM and THOR-50M model. The measurement locations for each model were set to compare the kinematics of the bodies during collision. The THOR-50M model has measurement locations at the head, the first, fourth and twelfth thoracic vertebrae (T1, T4, T12), and the pelvis. In the elderly HBM model, the head, first and ninth thoracic vertebrae (T1, T9), the second lumbar vertebra (L2) and the pelvis were set so as to be locations close to those of THOR-50M model. The origin of the coordinate system was set at a certain point without deformation in the vehicle body model.

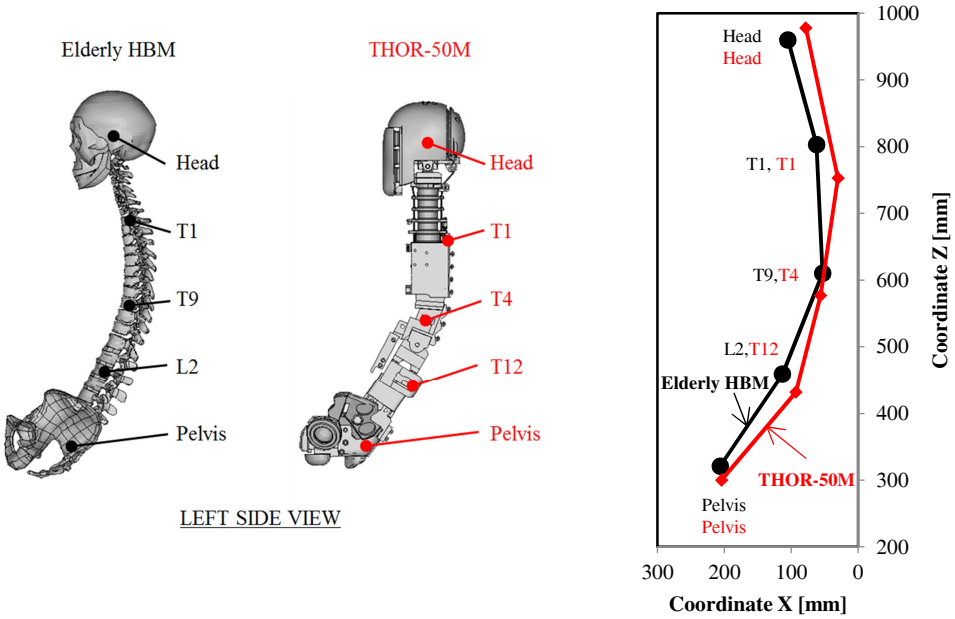

Figure 3. Measurement locations and posture of the elderly HBM and THOR-50M model

Figure 4 shows the measurement locations of thorax deformation of the elderly HBM and THOR-50M model. The 3D thorax deformations of THOR-50M's ribs were measured by the four equipped IR-TRACCs. Aiming at the

places closest to measurement locations of the THOR-50M, the thorax deformations of the elderly HBM were measured at four locations. The upper thorax deformations on both the left and right were measured between the 4th thoracic vertebrae and rib tips, and the lower thorax deformations on both the left and right were measured between the 8th thoracic vertebrae and rib tips.

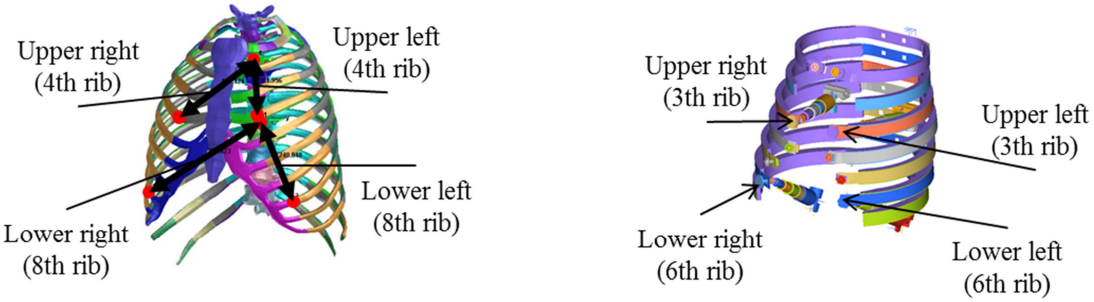

(a) Elderly HBM (b) THOR-50M model

Figure 4. Measurement locations of thorax deformation of the elderly HBM and THOR-50M model

RESULTS

Kinematics of occupant FE model

Figure 5 shows the displacement of the occupant FE models in each test condition. The X, Y, and Z axes were defined as the longitudinal, lateral and vertical directions of the vehicle coordinate system, respectively. For the elderly HBM, the displacement of the head, T1, T9, L2 and pelvis were shown, and for the THOR-50M model, the displacement of the head, T1, T4, T12 and pelvis were shown. The displacements of the occupant FE models until reaching its X-axis maximum at the vehicle coordinate system were shown in each test condition. The kinematics of each body component was in same trend between the elderly HBM and THOR-50M model in each test condition. In FWRB, between the elderly HBM and the THOR-50M model, the X-axis maximum displacement differences of the head and the pelvis were approximately 50mm or less. The X-axis maximum displacement of the thoracic vertebrae (T1, T4, T12) of THOR-50M model was less than those (T1, T9, L2) of the elderly HBM. In such cases with lateral vehicle motion as SOT and OMDB, between the elderly HBM and THOR-50M models, the X-axis maximum displacement difference of the pelvis was approximately 50mm or less. The X and Y-axis maximum displacements of the head and the thoracic vertebrae (T1, T4, T12) of THOR-50M model were less than those (head, T1, T9, L2) of the elderly HBM. Between the elderly HBM and THOR-50M models, the Y-axis maximum displacement differences of the head, thoracic vertebrae and pelvis were approximately 100 mm or less.

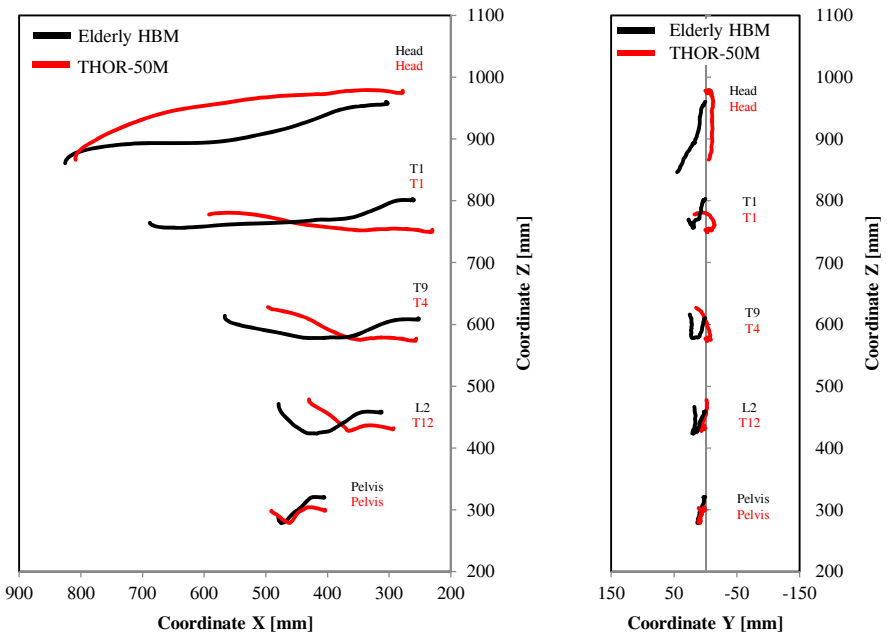
Elderly HBM
THOR-50M
Head
Head
T1
T1
T9
T4
L2
T12
Pelvis
Pelvis
Coordinate X [mm]
Coordinate Z [mm]
Coordinate Y [mm]
LEFT SIDE VIEW
REAR VIEW

(a) FWRB

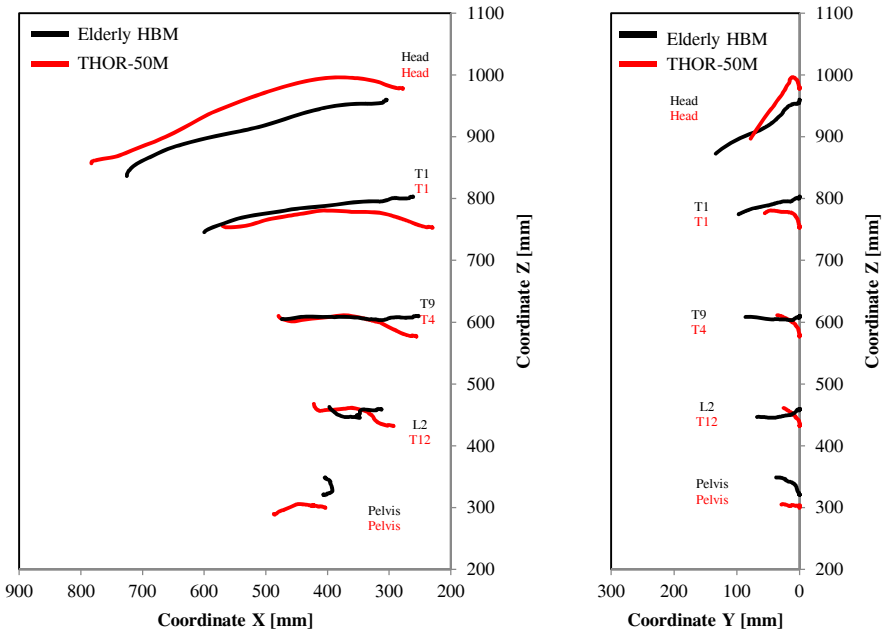
Elderly HBM
THOR-50M
Head
Head
T1
T1
T9
T4
L2
T12
Pelvis
Pelvis
Coordinate X [mm]
Coordinate Z [mm]
Coordinate Y [mm]
LEFT SIDE VIEW
REAR VIEW

(b) ODB

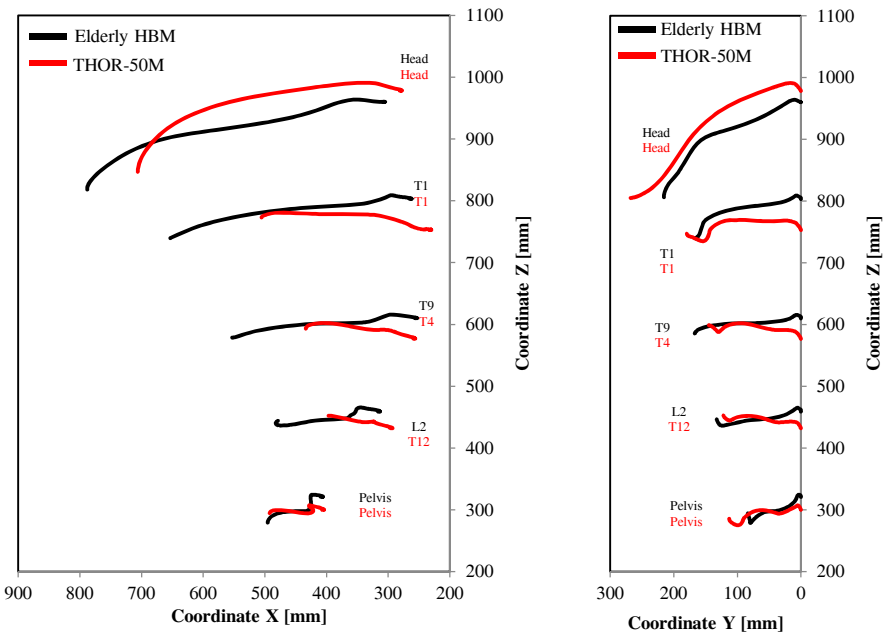

LEFT SIDE VIEW REAR VIEW

(c) SOT

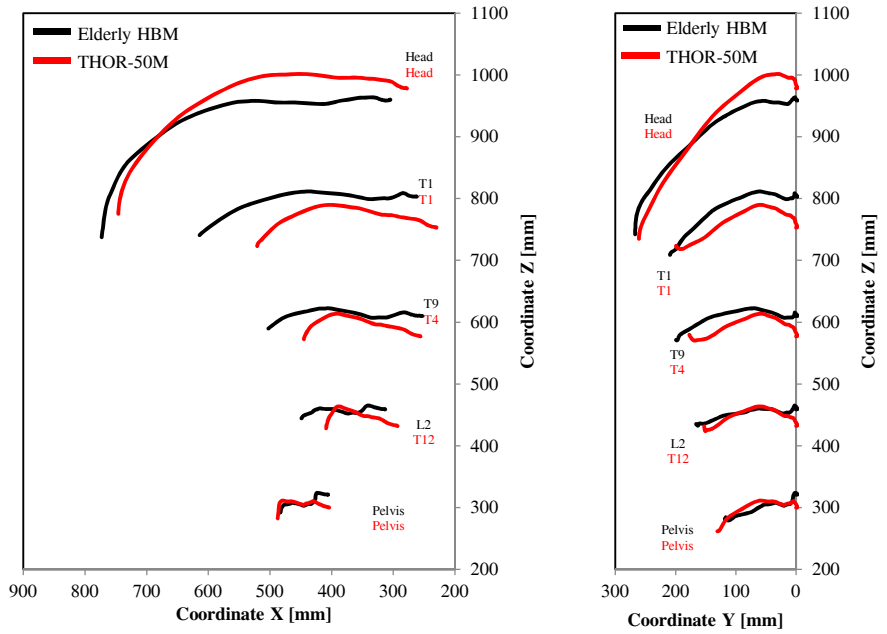

LEFT SIDE VIEW REAR VIEW

(d) OMDB

Figure 5. The displacements of the occupant FE models until reaching its X-axis maximum at the vehicle coordinate system in each test condition

Thorax deformation

Table 1 shows the maximum resultant thorax deformation of the elderly HBM and THOR-50M model in each test condition. Among all test conditions, the thorax deformation of the lower left in OMDB of the elderly HBM showed the maximum value. Figure 6 illustrates the deformed thorax shape and the displacement of the left 8th rib tip of the elderly HBM from the viewpoint fixed at the 8th thoracic vertebra at 0 ms and 105 ms in OMDB. It was observed the expansion of a part of the rib cage appeared that was caused by an inertial force from the abdominal parts moving forward and by an excessive flexion of the trunk during the rebound phase in the crash. Since such a phenomenon of the human model has not been validated and could not be related with thorax deformation, these thorax deformations were omitted from the discussion hereafter in this research and denoted by parentheses in Table 1. For the elderly HBM and THOR-50M model in all test conditions, the thorax deformation at the upper right was largest among the four measurement locations.

Table 1.
Maximum thorax deformation of the elderly HBM and THOR-50M models at four measurement locations in each test condition

	Maximum resultant thorax deformation (mm)							
	Upper right		Upper left		Lower right		Lower left	
Test conditions	Elderly HBM	THOR-50M model	Elderly HBM	THOR-50M model	Elderly HBM	THOR-50M model	Elderly HBM	THOR-50M model
FWRB	55.9	40.4	33.3	17.1	22.9	30.2	43.8	12.7
ODB	53.6	36.5	32.7	17.0	25.4	31.3	46.5	11.5
SOT	56.6	42.0	35.0	17.4	26.6	35.2	49.3	13.9
OMDB	58.0	50.7	52.5	27.5	(50.9)	35.8	(85.4)	25.0

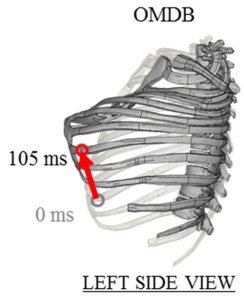

Figure 6. The deformed thorax shape and the displacement of the left 8th rib tip (Arrow) of the elderly HBM from the viewpoint fixed at the 8th thoracic vertebra at 0 ms and 105 ms in OMDB

The thorax deformations were measured at four locations (upper right, upper left, lower right, lower left) for the elderly HBM and THOR-50M model. The correlations of thorax deformation in resultant (Res.), X, Y and Z-axis between the elderly HBM and THOR-50M model at four measurement locations were investigated in all test conditions. As an example, Fig. 7 plots the thorax deformation every 5 ms until either the thorax deformation of the elderly HBM or THOR-50M model have reached its maximum at the upper right thorax in FWRB. The R^2 (correlation coefficient) and the ratio of variability of the approximation straight line that passed the origin were calculated from all results. Figure 8 shows the R^2 of zero or more between the elderly HBM and THOR-50M models, and Fig. 9 shows the ratio of the thorax deformation of the THOR-50M model to that of the elderly HBM, at four locations in each test condition. When focusing on the upper right thorax deformation where there was maximum deformation in all test conditions, the Res., X-axis, and Z-axis thorax deformation had high correlation between the elderly HBM and THOR-50M model. In the upper right thorax deformation, the ratio of variability in X-axis was larger than 1, in Z-axis it was less than 1. In other words, in X-axis the thorax of the THOR-50M model was easier to deform than that of the elderly HBM, in Z-axis it was not. In Y-axis thorax deformation between them didn't show a good correlation. In Y-axis the thorax of THOR-50M model wasn't easier to deform than that of the elderly HBM. In contrast, in the lower left thorax where the belt did not pass directly, there was a low correlation between

them in Res. and all axes. It may be because of too little deformation of both to statistically show a certain correlation.

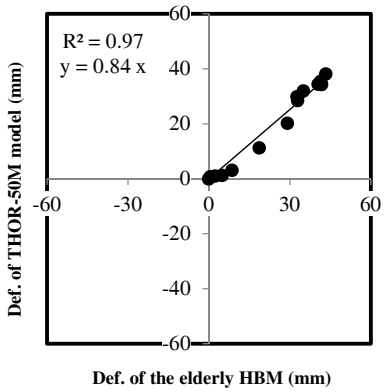

Figure 7. The plots of the thorax deformations every 5 ms until either the thorax deformation of the elderly HBM or THOR-50M model reached the maximum value at the upper right thorax in FWRB

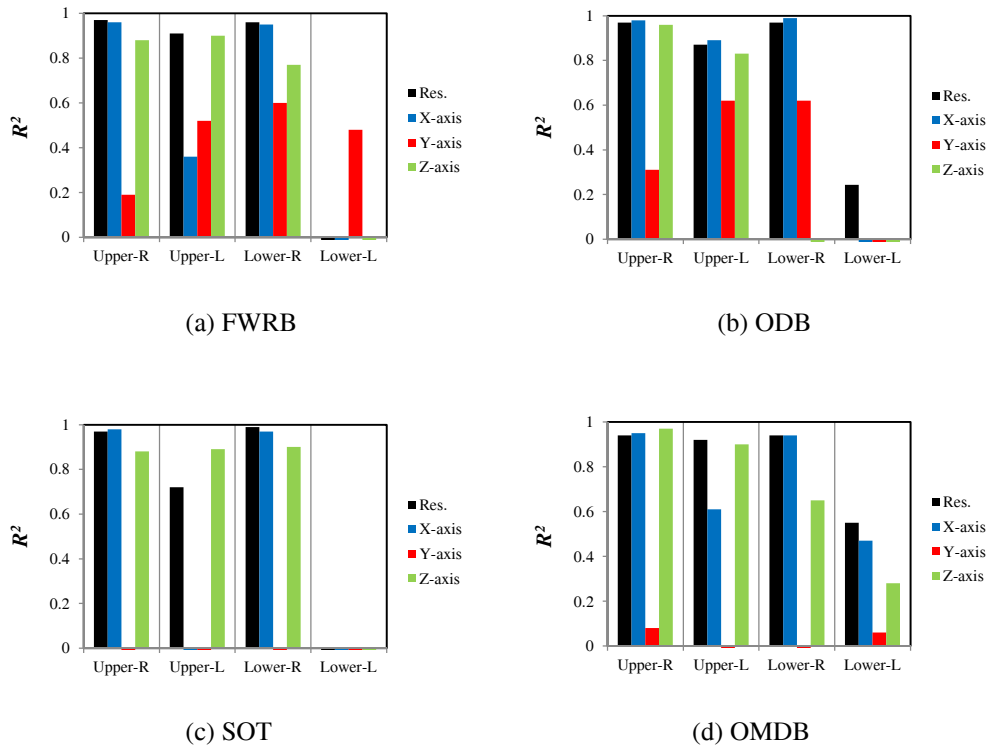

(a) FWRB (b) ODB

(c) SOT (d) OMDB

Figure 8. The R^2 of zero or more between the thorax deformation of the elderly HBM and THOR-50M model in each test condition

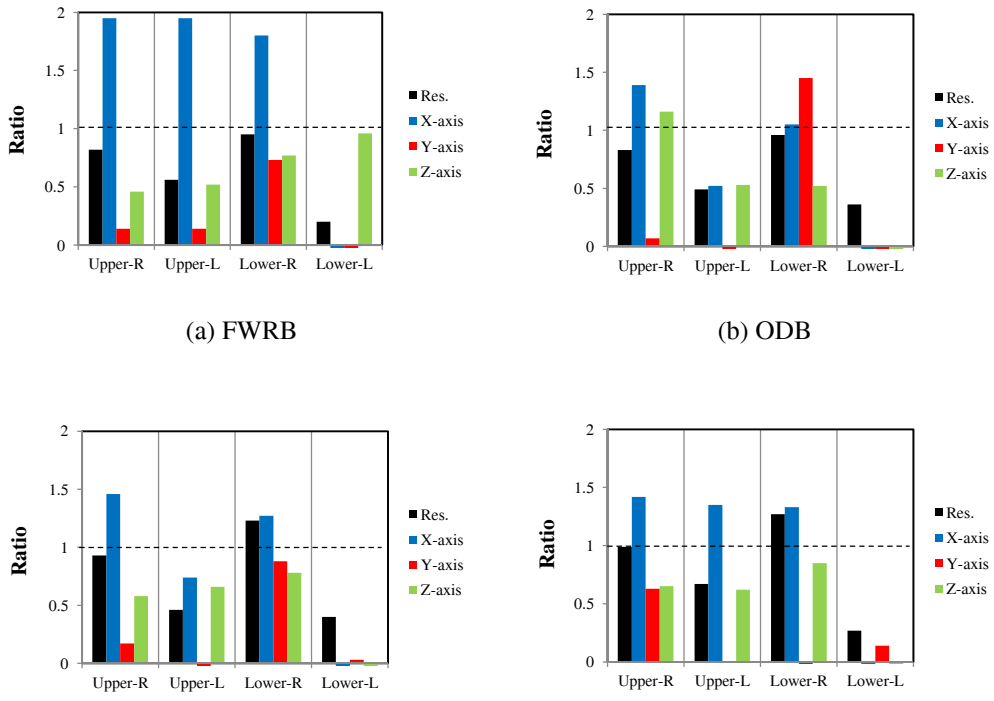

(a) FWRB (b) ODB

(c) SOT (d) OMDB

Figure 9. The ratio of the thorax deformation of the THOR-50M model to that of the elderly HBM in each test condition

Rib fractures of the elderly HBM

Figure 10 illustrates the locations of rib fracture of the elderly HBM in FWRB, ODB, SOT and OMDB. The locations of rib fracture were counted until reaching the maximum thorax deformation of the elderly HBM. In FWRB, the number of fractured ribs was 8 and there were fractured ribs around the right and left shoulder belt path. Both the left and right side ribs were fractured around the lateral. In ODB the number of fractured ribs was 4, the least among the four test conditions, and only left side ribs were fractured. The locations of fractured ribs in SOT were almost same as those in ODB;, in addition, the 9th and 10th ribs of the left side were also fractured. In OMDB the number of fractured ribs was 11 and the largest among the four test conditions. The locations of the fractured ribs were almost same as those of FWRB;, in addition, the 9th and 10th ribs of the left side were also fractured, like SOT. The 1st and 2nd ribs of the right side and the 6th rib of the left side were fractured but happened during the rebound phase after maximum excursion by upward loading from abdominal parts caused by extreme flexion of the body. Since such a phenomenon of the human model has not been validated and could not be related with thorax deformation, these fractures were omitted from the discussion hereafter in this research.

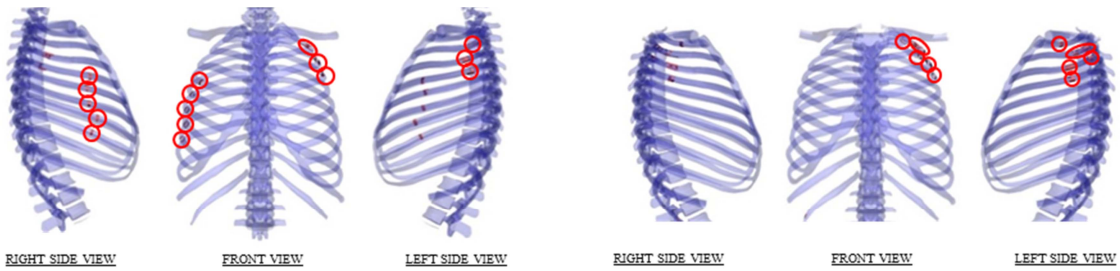

(a) FWRB (b) ODB

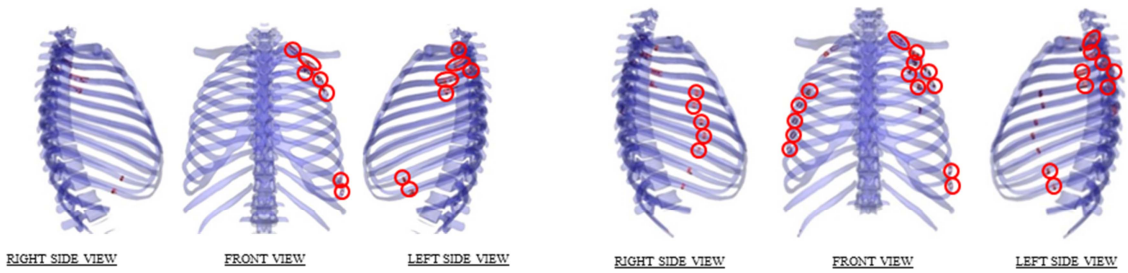

(c) SOT (d) OMDB

Figure 10. The locations of rib fractures of the elderly HBM in each test condition

The correlation between the number of the fractured ribs of the elderly HBM and R_{max} of THOR-50M model

From Fig. 10 the locations of rib fracture were roughly assorted into three regions on ribcage (Region A: the 1st to 8th ribs of left side; Region B: the 1st to 10th ribs of right side; and Region C: the 9th to 10th ribs of left side) as shown in Fig. 11. The correlation between the number of fractured ribs in all regions or each region and R_{max} was investigated.

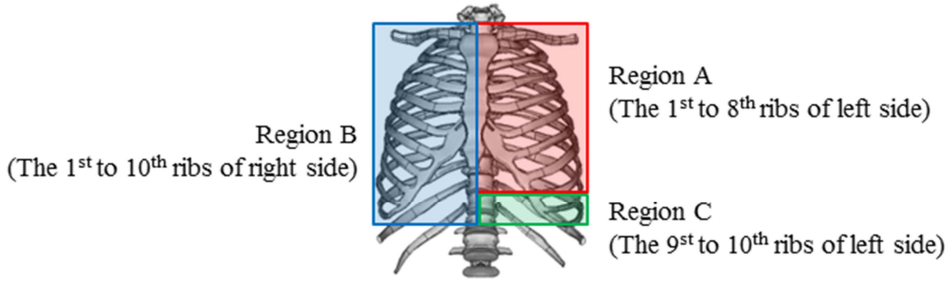

Figure 11. The assorted regions of the ribcage of the elderly HBM to classify the rib fracture locations

Figure 12 plots the number of the fractured ribs of the elderly HBM in all regions or each region and the R_{max} of THOR-50M model. The R^2 between them was calculated from the results of FWRB, ODB, SOT and OMDB. The R^2 in rib fractures of all regions was high as 0.84, while that of each region wasn't high as 0.7 or less.

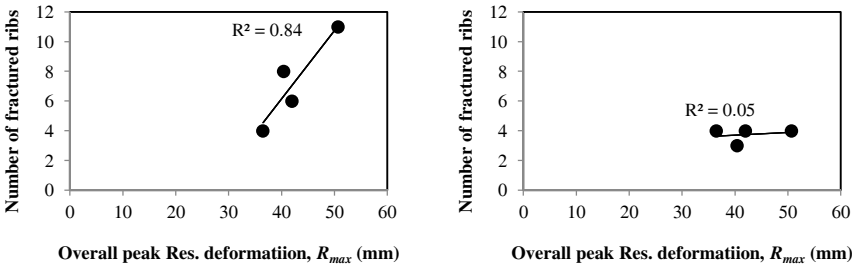

(1) All regions (2) Region A

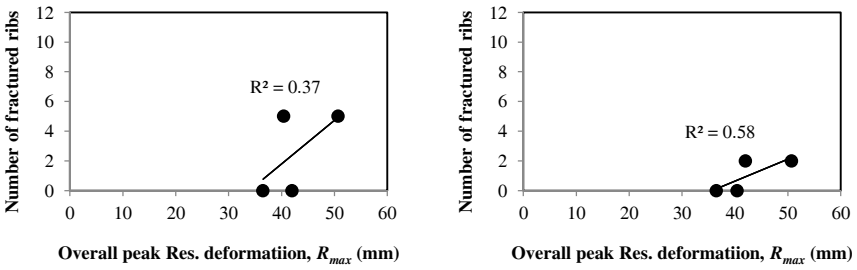

(3) Region B (4) Region C

Figure 12. The correlation between the number of the fractured ribs of the elderly HBM in all regions or each region and the R_{max} of THOR-50M model

DISCUSSION

As the result of Table 1, the measurement location of R_{max} was upper right in all test conditions. In the elderly HBM, the locations of rib fractures were not only around the upper right thorax but also the other thorax areas such as the upper left, lower right and lower left. Therefore, it was analyzed why the rib fractures of the elderly HBM occurred in each region.

Upper left rib fractures (Region A)

As shown in Fig. 10 and Fig. 11, there were the rib fractures of Region A in all test conditions. At the deformation measurement location of the upper left thorax close to the Region A, the ratio of the Res. thorax deformation of THOR-50M model to that of the elderly HBM was low although the correlation of the Res. thorax deformation between them was high, as shown in Fig. 8 and Fig. 9. In order to investigate this reason, these kinematics and thorax responses were compared. Fig. 13 shows the thorax responses of the elderly HBM and THOR-50M model from the viewpoint of the vehicle coordinate system during the SOT collision. It was observed that the clavicle and shoulder of the elderly HBM went down by the shoulder belt loading, while those of the THOR-50M model didn't. The human shoulder is connected to the thorax with the ligaments, muscles and so on. Therefore the shoulder can probably move in a wide range. It was presumed the upper ribs were fractured by the downward and rearward loading by the shoulder belt via the clavicle. Since it hasn't been investigated whether this phenomenon occurs in a real human body, the rib fractures may be peculiar to this elderly HBM. In THOR-50M, structurally the shoulder can move limitedly within a certain range. It was thought that it was hard for the shoulder belt loading to be transmitted from the shoulder to the ribcage because the loading was transmitted from the shoulder to the spine. By these reasons, the upper left deformation of the THOR-50M model might be less than that of the elderly HBM.

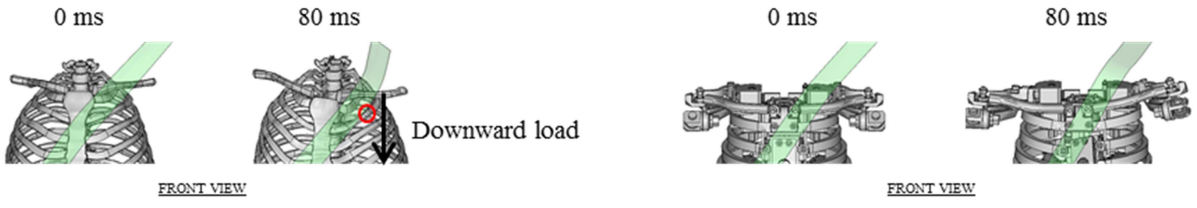

(a) Elderly HBM (b) THOR-50M model

Figure 13. The illustration of the thorax response of the elderly HBM from the viewpoint of the vehicle coordinate system during the SOT collision

Upper and lower right rib fractures (Region B)

As shown in Fig. 10 and Fig. 11, the number of fractured ribs of Region B was much different depending on the test conditions. The rib fractures of Region B occurred in FWRB and OMDB, but none did in ODB and SOT. The correlation between the number of fractured ribs of Region B and the R_{max} of THOR-50M model wasn't high as 0.37, as shown in Fig. 12. In order to investigate this reason, the thoracic kinematics and the deformed thorax of the elderly HBM during collision were observed. Figure 14 shows the trajectories of the 9th thoracic vertebra of the elderly HBM in X-Y plane until reaching the X-axis maximum displacement at the vehicle coordinate system in all test conditions with marking the timing when right side rib fractures have all happened in FWRB and OMDB or the thorax deformation have reached its maximum in ODB and SOT. Among the crash test conditions including lateral vehicle motion such as ODB, SOT and OMDB, the Y-axis displacement of the 9th thoracic vertebra in OMDB was least at each time. Figure 15 illustrates the deformed thorax shape and the shoulder belt path of the elderly HBM from the viewpoint fixed at the 4th thoracic vertebra at the time when right side rib fractures have all happened in FWRB and OMDB or the thorax deformation have reached its maximum in ODB and SOT. The θ represents the angle between the direction of the lower right shoulder belt and the X-axis in X-Y plane of the 4th vertebra. Each time, the θ in FWRB, ODB, SOT and OMDB were respectively defined as θa, θb, θc and θd. The θa and θd (in FWRB and OMDB) were less than θb and θc (in ODB and SOT). Therefore, it was assumed that the forward deceleration of the vehicle in FWRB and OMDB was larger than that in ODB and SOT, and the rearward loading by the shoulder belt to the thorax was applied more due to the occupant moving in the forward direction. When the X component of the shoulder belt load to thorax is large, there may be a possibility that rib fracture tends to occur. It may be necessary to further study the influence that the direction and magnitude of input to the thorax has on the severity of rib fractures.

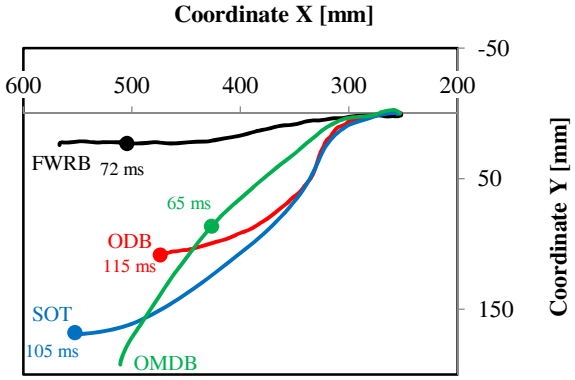

Figure 14. The trajectories of the 9th thoracic vertebra of the elderly HBM in X-Y plane until reaching the X-axis maximum displacement at the vehicle coordinate system in all test conditions with marking the timing when right side rib fractures have all happened in FWRB and OMDB or the thorax deformation have reached its maximum in ODB and SOT

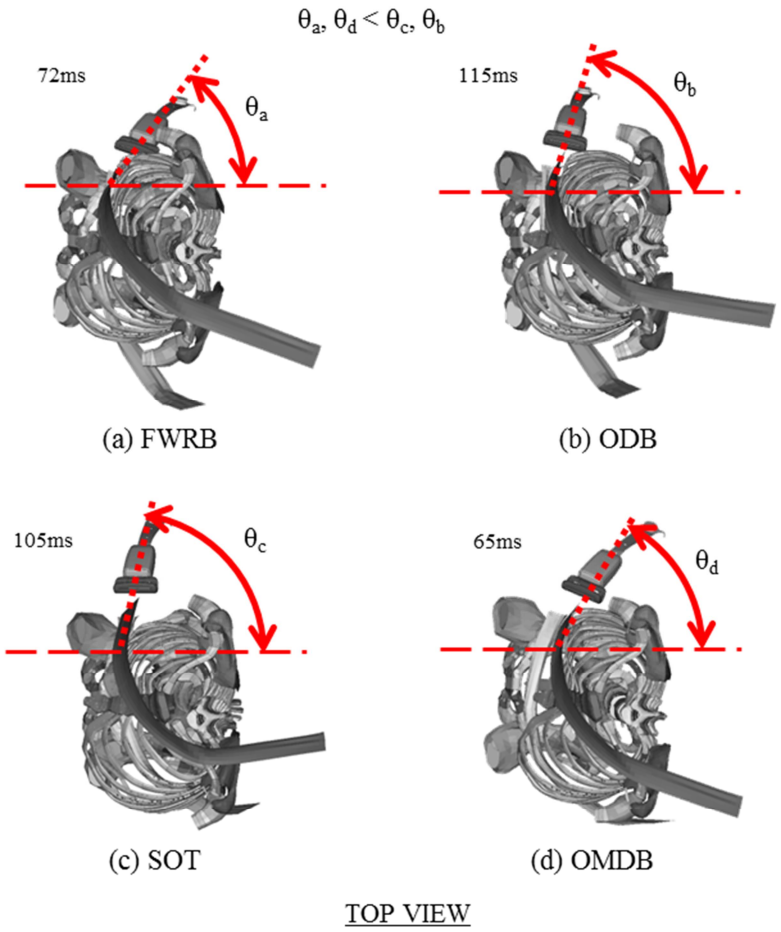

Figure 15. The deformed thorax shape and the shoulder belt path of the elderly HBM from the viewpoint fixed at the 4th thoracic vertebra at the time when right side rib fractures have all happened in FWRB and OMDB or the thorax deformation have reached its maximum in ODB and SOT, with θ representing the angle between the direction of the lower right shoulder belt and the X-axis in the vehicle X-Y coordinate of the 4th thoracic vertebra

Lower left rib fractures (Region C)

As shown in Fig. 10, the ribs around the lower left thorax were fractured in such cases including the lateral vehicle motion as SOT and OMDB. It was observed that the thorax of the elderly HBM contacted the door trim although that of THOR-50M model didn't. The difference of thorax response between the elderly HBM and THOR-50M models is considered to have occurred for following reasons:

Firstly, there was the difference of the thorax maximum displacement in Y-axis between the elderly HBM and THOR-50M models. As shown in Fig. 5, the Y-axis maximum displacements of the thoracic vertebrae (T1, T9, L2) of the elderly HBM were larger than those (T1, T4, T12) of the THOR-50M model in SOT and OMDB. Figure 16 shows the deformed body shapes of the elderly HBM and THOR-50M model and the door trim from the viewpoint of the vehicle coordinate system at 94ms in SOT. The spine of the elderly HBM was curved more outward than that of THOR-50M model. The human spine consists of multiple vertebrae and intervertebral discs. In the elderly HBM, that enables such a flexible motion. In contrast, THOR-50M has only the upper thoracic spine flex joint and lumbar spine flex joint made of rubber as components of the spine. Therefore, it was considered that the spine of the THOR-50M model could bend limitedly.

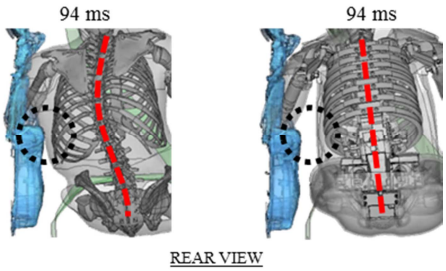

Figure 16. The deformed body shapes and the door trim from the viewpoint of the vehicle coordinate system in SOT

Secondly, there is the difference of the thorax geometry between the elderly HBM and THOR-50M model as shown in Fig. 17. The rib cage of the elderly HBM was created based on the CAD of one elderly individual with the body size close to AM50%ile by Ito et al. [3]. Its geometry showed it had a bit wider around the lower part and a higher bottom than THOR-50M; that made the elderly HBM contact the door trim while THOR-50M didn't reach it.

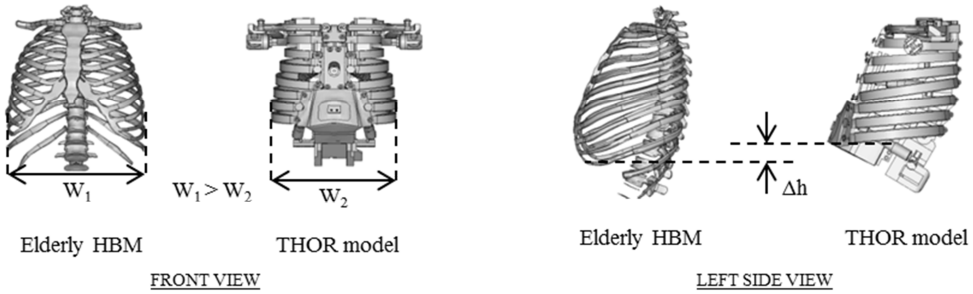

Figure 17. The thorax geometry of the elderly HBM and THOR-50M model

Thirdly, between the elderly HBM and THOR-50M model there was the thorax response difference around the lower left where the shoulder belt didn't pass directly. Figure 18 shows the deformed thorax shapes of the elderly HBM and THOR-50M models from the viewpoint fixed at the 4th thoracic vertebra at 0 ms and 70 ms in SOT. In the elderly HBM, it was observed that the rib cage around the lower left was swollen largely. It is assumed that the forward inertial force of the viscera contributed to this phenomenon. In the THOR-50M model, it is thought that the rib cage hadn't been swollen because THOR-50M has no part simulating human viscera. At the lower left thorax, the correlation of the thorax deformation between the elderly HBM and THOR-50M model might not be high due to the difference of the inertial force by the viscera.

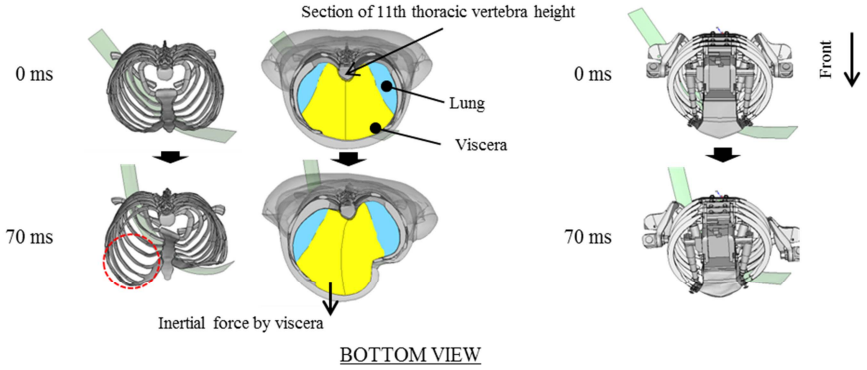

(a) Elderly HBM (b) THOR-50M model

Figure 18. The deformed thorax shapes from the viewpoint fixed at the 4th thoracic vertebra at 0 ms and 70 ms in SOT

Mainly for these three reasons, it was consider that the distance between the thorax of the elderly HBM and the door trim decreased during the collision in SOT and OMDB. The thorax contact to the door trim occurred, and the ribs around the lower left ribs were fractured. The rib fractures and thorax response may be peculiar to this elderly HBM since it hasn't been investigated whether this phenomenon occurs in a real human body.

CONCLUSION

In this research, the comparison of the thorax response between human and THOR-50M under simulated frontal crashes including lateral vehicle motion such as FWRB, ODB, SOT and OMDB was performed, that showed a certain correlation between rib fractures of the elderly HBM and the thorax deformation of THOR-50M. As the results, the following conclusion was obtained.

- For the elderly HBM and THOR-50M model in all the test conditions, the thorax deformation at the upper right was largest among four measurement locations, and that of the elderly HBM and THOR-50M model showed good correlation.
- The number of fractured ribs of the elderly HBM and the overall peak resultant deformation (R_{max}) of THOR-50M model calculated in four crash test conditions showed good correlations. However, the number of the fractured ribs assorted into three regions didn't show a good correlation with R_{max}.
- The upper left ribs of the elderly HBM were fractured by the downward and rearward loading by the shoulder belt via the clavicle. In the THOR-50M model, however, because the shoulder can move within a structurally limited range, such a mechanism of deformation could not be represented.
- A few of right ribs were fractured in FWRB and OMDB, and none was in ODB or SOT. Under the condition of FWRB or OMDB where the occupant moves more forward than ODB or SOT by higher frontal deceleration, there may be a possibility that rib fractures occur due to the higher rearward loading by shoulder belt to the thorax.
- A few of the lower left ribs were fractured in SOT and OMDB because the thorax contacted the door trim in the elderly HBM, while it didn't in the THOR-50M model.

The results of this study suggested that the R_{max} of THOR-50M might be an acceptable index to evaluate an overall severity for the occupant thorax in frontal crash conditions while further study for the methods to evaluate detailed thorax injury using THOR-50M should be needed in order to correlate any other indices and possible thorax injuries in the crash condition with lateral motion. At the current status, when the current THOR-50M measurements are used to evaluate the injury risk, it is important to understand such the characteristics above.

REFERENCES

[1] National Police Agency, 'Traffic Accident Situation', http://www.e-stat.go.jp (2016)

[2] Shimamura M, Ohhashi H, Yamazaki M, 'The Effects of Occupant Age on Patterns of Rib Fractures to Belt-Restrained Drivers and Front Passengers in Frontal Crashes in Japan', Stapp Car Crash Journal, Vol. 47 (October 2003), pp.349-365

[3] Ito, O., Dokko, Y., Ohashi, K., 'Development of Adult and Elderly FE Thorax Skeletal Models', SAE Technical Paper 2009-01-0381, 2009, doi:10.4271/2009-01-0381

[4] Rangarajan, Shams, T.,N.,White, R., Oster, J, Hjerpe, E., Haffner, 'Response of THOR in Frontal Sled Testing in Different Restraint Conditions', IRCOBI Conference Proceedings, (Sept. 1998)

[5] Xu L, Jensen J, Brynes K, Kim A, Agaram V, Davis K, Hultman R, Kostyniuk G, Marshall M, Mertz H, Nusholtz G, Rouhana S, Scherer R., 'Comparative performance evaluation of THOR and Hybrid II', SAE paper no. 2000-01-0161 SAE, Warrendale, PA. (2000)

[6] Richard Kant, Greg Shaw, David Lessley, Jeff Crandall, Dimitris Kallieris, Mats Svensson, 'Comparison of Belted Hybrid III, THOR, and Cadaver Thoracic Responses in Oblique Frontal and Full Frontal Sled Tests', SAE Technical Paper, 2003-01-0160, p. 1-16, (2003)

[7] Greg Shaw, David Lessley, Joe Ash, Jeff Crandall, Dan Parent, 'Response Comparison for the Hybrid III, THOR Mod Kit with SD-3 Shoulder, and PMHS in a Simulated Frontal Crash', Proceeding of the 23rd ESV Conference, Report No.13-0130, (2013)

[8] Devon L Albert, Stephanie M Beeman, and Andrew R Kemper, 'Assessment of Thoracic Response and Injury Risk Using the Hybrid III, THOR-M, and Post-Mortem Human Surrogates under Various Restraint Conditions in Full-Scale Frontal Sled Tests', Stapp Car Crash Journal, Vol. 62 (November 2018), pp. 1-65

[9] Ito, O., Dokko, Y., Ohashi, K., 'Development of the Human Lower Limb FE Models of Adult and Elderly Person Considering Aging Effects', Proceedings, JSAE Annual Congress (Spring), #20085048 (2008)

[10] Dokko, Y., Ito, O., and Ohashi, K., "Development of Human Lower Limb and Pelvis FE Models for Adult and the Elderly," SAE Technical Paper 2009-01-0396 (2009), doi: 10.4271/2009-01-0396.

[11] Dokko, Y., Kanayama, Y., Ito, O., and Ohashi, K., "Development of Human Lumbar Spine FE Models for Adult and the Elderly," SAE Technical Paper 2009-01-0382 (2009), doi:10.4271/2009-01-0382.

[12] Humanetics Innovative Solutions : THOR-50th Metric V1.4.1 LS-DYNA Model Technical Report User's Manual, (2016)

[13] LSTC : LS-DYNA Version 971 R6 User's Manual, (2012)

[14] National Highway traffic Safety Administration, 'Oblique Test Procedure', Docket ID 2015-0119, (2016)